Computers in Biology and Medicine 86 (2017) 75–81

Contents lists available at ScienceDirect

Computers in Biology and Medicine

journal homepage: www.elsevier.com/locate/compbiomed

Influence of different frequencies of axial cyclic loading on time-domain vibration response of the lumbar spine: A finite element study

Wei Fan, Li-Xin Guo*

School of Mechanical Engineering and Automation, Northeastern University, Shenyang, PR China

ARTICLE INFO

Keywords:
Axial cyclic loading
Different frequencies
Finite element
Follower preload
Lumbar spine
Resonance
Time-domain
Whole-body vibration

ABSTRACT

Very few studies have quantitatively analyzed influence of the loading frequency on time-domain vibration response of the whole lumbar spine in the presence of a physiologic compressive preload. In this study, a three-dimensional non-linear finite element model of ligamentous L1–S1 segment was developed to predict time-domain dynamic response of the whole lumbar spine to axial cyclic loading with different frequencies. A compressive follower preload of 400 N was applied to the model to simulate the physiologic compressive load. Modal analysis was initially performed to extract axial resonant frequency of the model under a 40 kg upper body mass and the 400 N preload. The result showed that the axial resonant frequency was 7.77 Hz. Subsequently, transient dynamic analyses were performed on the model under a sinusoidal axial load of ±40 N at frequencies of 3, 5, 7, 9, 11, 13 and 15 Hz with the 400 N preload and 40 kg mass. The computational results (strains and stresses in the spinal components) were collected and plotted as a function of time. These predicted results were found to be frequency-dependent and consistent with the notion in engineering dynamics texts that the closer the loading frequency approaches the resonant frequency, the larger the response is. For example, the results for 5 Hz load compared to 3 Hz load showed a 68.6–111.5% increase in peak-to-bottom variations of the predicted response parameters, and the results for 13 Hz load compared to 11 Hz load showed a 26.4–37.8% decrease in these variations.

1. Introduction

There appears to be a strong link between occupational whole-body vibration (WBV) exposure and low back pain [1–3]. The cyclic loading encountered due to the WBV exposure has been shown to significantly contribute to the low back disorders [4]. Experimental studies have indicated that exposure of the human lumbar spine to cyclic loading may cause microfracture in the bone and endplate and microlesion in the intervertebral disc [5,6], which could result in fatigue fracture of the spine structure and low back problems. To quantitatively describe impact of the cyclic loading on the spine, the strain and stress in spinal components need to be evaluated. However, these are difficult or even impossible to achieve by experimental methods. By contrast, the finite element (FE) strategy provides an alternative method for solving the problem.

Several FE models have been proposed to investigate time-domain dynamic response of the lumbar spine to the axial cyclic loading during WBV. For example, Goel et al. [7] developed a L4–S1 model to compare the response values of stresses and strains in the spine for a sinusoidal axial load with the corresponding results for axial static load (with equivalent magnitude). They concluded that the cyclic load was more dangerous than static load. Guo et al. [8] developed a L3–L5 model with various injury conditions and investigated dynamic response of the injured lumbar spine to the sinusoidal axial load. They found that the injuries exacerbated the intervertebral disc degeneration under the cyclic loading condition. Although these previous studies have given valuable insights into time-domain behavior of the lumbar spine on the condition of cyclic loading, the employed FE models of short motion segments were unadvantageous to reflect dynamic characteristics of the whole lumbar spine.

Accordingly, in this study, the authors attempted to develop a FE model of the L1–S1 motion segment subjected to the physiologic loading condition for predicting time-domain dynamic response in lumbar region to the axial cyclic loading. In order to better understand the impact of the cyclic loading on the lumbar spine, the individual effect of the factors that characterize the cyclic loading should be isolated, and there are three key factors: frequency, amplitude and duration [9,10]. This study would focus on the frequency effect.

* Corresponding author. School of Mechanical Engineering and Automation, Northeastern University, No. 3-11, Wenhua Road, Heping District, Shenyang, 110819, PR China.
E-mail address: lxguo@mail.neu.edu.cn (L.-X. Guo).

http://dx.doi.org/10.1016/j.compbiomed.2017.05.004
Received 18 January 2017; Received in revised form 7 May 2017; Accepted 7 May 2017

2. Materials and methods

2.1. FE modeling

The three-dimensional FE model was generated in ABAQUS software (version 6.10), based on computed tomography (CT) scans of the spinal segment L1–S1 of an asymptomatic 48-year-old female (162 cm and 58 kg) (Fig. 1). Each vertebra consisted of a cancellous bone surrounded by a 0.7 mm endplate and cortical shell [11]. Each intervertebral disc consisted of a nucleus pulposus surrounded by an annulus ground substance comprising six fiber layers with crosswise pattern close to ±30° [12]. The fluidlike behavior of the disc was assumed to be nearly incompressible and governed by hyperelastic Mooney-Rivlin material law [13]. The facet joint contacts were defined as surface-to-surface contact elements with no friction [12,13]. Seven spinal ligaments (anterior longitudinal (ALL), posterior longitudinal (PLL), flavum (FL), supraspinous (SSL), interspinous (ISL), intertransverse (ITL) and capsular (JC) ligaments) were included in the model. The material properties used in present study for various tissues were taken from the literature [13–17] and listed in Tables 1 and 2. The model was validated against the experimental data available in the literature [18–20], and the model predictions were also compared with the published numerical results [21].

2.2. Boundary and loading conditions

The caudal part of the sacrum was fixed in all directions. To simulate the physiologic compressive load on the whole lumbar spine induced by muscle contraction, a compressive follower preload of 400 N was applied to the model along a path that approximates the tangent to the spinal curve [22] using placed bilaterally thermo-isotropic truss elements [19] (Fig. 1). Fig. 2 illustrated the shape of the spine model loaded with the 400 N preload, which produced maximum rotations of 0.75° in the sagittal, 0.26° in the coronal and 0.19° in the transverse planes. As suggested by Renner et al. [19], the intervertebral rotation caused by the compressive follower preload should be less than 1°. Therefore, it indicated that the preload had been appropriately applied to the present FE model. Then, this state would be propagated and used as an initial condition for the modal and transient dynamic analyses.

Modal analysis was initially performed to extract axial resonant frequency of the L1–S1 model considering an upper body mass of 40 kg, which was simulated by applying a mass point of 40 kg to the top of L1 by 1 cm anterior to the L3–L4 vertebral centroid [23,24]. Subsequently, transient dynamic analyses were performed on the model (including the

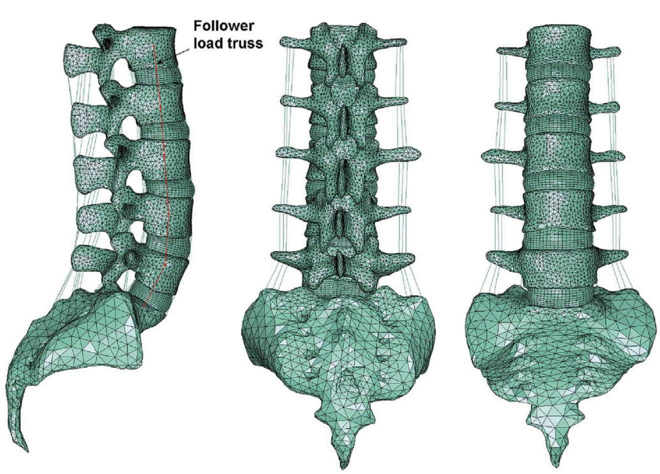

Fig. 1. FE model of the whole lumbar spine L1–S1 with the application of a compressive follower preload using thermo-isotropic truss elements attached bilaterally to the cortical shell of the vertebrae.

Table 1
Material properties for the bones and the intervertebral disc of the FE model.

Material	Element type	Young's modulus (MPa)	Poisson ratio	Density (Kg/mm³)	References
Bones					
Cortical bone	S3	12000	0.3	1.7×10^{-6}	[14]
Cancellous bone	C3D4	100	0.2	1.1×10^{-6}	[14]
Posterior bone elements	C3D4	3500	0.25	1.4×10^{-6}	[14]
Endplate	S3	23.8	0.4	1.2×10^{-6}	[15]
Intervertebral disc	C3D8				[13]
Annulus ground substance		Hyperelastic, Mooney-Rivlin $C_{10} = 0.18$, $C_{01} = 0.045$		1.05×10^{-6}	
Nucleus pulposus		Hyperelastic, Mooney-Rivlin $C_{10} = 0.12$, $C_{01} = 0.03$		1.02×10^{-6}	

S3, 3-node triangular elements; C3D4, 4-node tetrahedral elements; C3D8, 8-node hexahedral elements.

Table 2
Material properties for the annulus fibers and the ligaments of the FE model.

Material	Element type	Young's modulus (MPa)	Cross-sectional area (mm2)	Density (Kg/mm³)	References
Annulus fiber layers	Tension-only T3D2				[16]
Outermost		550	0.7	1.0×10^{-6}	
Second		495	0.63	1.0×10^{-6}	
Third		440	0.55	1.0×10^{-6}	
Fourth		420	0.49	1.0×10^{-6}	
Fifth		385	0.41	1.0×10^{-6}	
Innermost		360	0.30	1.0×10^{-6}	
Ligaments	Tension-only T3D2				[17]
ALL		7.8(<12.0%), 20(>12.0%)	63.7	1.0×10^{-6}	
PLL		10.0(<11.0%), 20(>11.0%)	20	1.0×10^{-6}	
FL		15.0(<6.2%), 19.5(>6.2%)	40	1.0×10^{-6}	
SSL		8.0(<20.0%), 15(>20.0%)	30	1.0×10^{-6}	
ISL		10.0(<14.0%), 11.6(>14.0%)	40	1.0×10^{-6}	
ITL		10.0(<18.0%), 58.7(>18.0%)	1.8	1.0×10^{-6}	
JC		7.5(<25.0%), 32.9(>25.0%)	30	1.0×10^{-6}	

T3D2, 2-node truss elements.

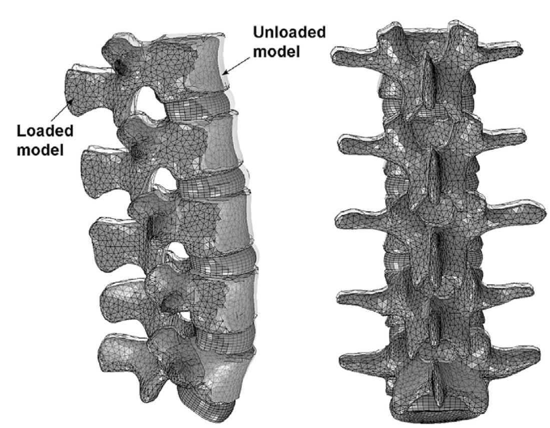

Fig. 2. Shape of the lumbar spine (sacrum was not shown) under a compressive follower preload of 400 N.